NUMERICAL UNCERTAINTY ESTIMATION IN MARITIME CFD APPLICATIONS

CHRISTIAAN M. KLAIJ[*,1], GUILHERME VAZ[1] AND LUÍS EÇA[2]

[1] Maritime Research Institute Netherlands, P.O.Box 28, 6700AA Wageningen, The Netherlands, c.klaij@marin.nl, g.vaz@marin.nl, http://www.marin.nl/
[2] Instituto Superior Técnico, Av. Rovisco Pais 1, 1049-001 Lisboa, Portugal, luis.eca@ist.utl.pt, http://tecnico.ulisboa.pt/

Key words: computational fluid dynamics, verification and validation, uncertainty estimation, maritime applications.

Abstract. The results of a numerical uncertainty estimation procedure are presented for a variety of industrial CFD applications with a finite volume RaNS solver. The numerical uncertainty estimation is indispensable when assessing the reliability of CFD results. Highly-refined grids and good iterative convergence are required to obtain global quantities such as force coefficients with a numerical uncertainty of a few percent.

1 INTRODUCTION

The availability of computer power and computational fluid dynamics (CFD) software, both commercial and open-source, has led to routine use of CFD simulations in maritime industry in the design of ships and offshore structures. The steady, incompressible Reynolds-averaged Navier-Stokes (RaNS) equations are mostly used, discretized by co-located finite-volume methods for (un)structured, body-fitted grids. Simulations with this model provide detailed flow fields that can help in diagnosing problems, improving designs and studying scale effects.

However, before making any design decisions, the reliability of such simulations needs to be established. This takes three steps – Code Verification, Solution Verification and Validation [1, 2]. Code verification comes first as it ensures that the model is correctly implemented in a given software package. Solution Verification then provides an uncertainty interval ('error bar') on a specific simulation result. Finally, Validation compares simulation results to experimental results, both with error bars, i.e. within a given validation uncertainty, to check that the model is adequate for the problem at hand.

In this paper, we focus on Solution Verification with the numerical uncertainty estimation procedure proposed in [3] which is used at the Maritime Research Institute Netherlands (MARIN). Similar procedures, for example [4, 5], are used elsewhere to provide error bars of simulation results. These error bars allow the CFD engineer to assess

1

the reliability of the results and make informed design decisions. A numerical uncertainty of a few percent can be acceptable, depending on the purpose. For example, in applications related to resistance and propulsion of ships, an uncertainty of 1% is desired while in applications related to wind and current loads on offshore structures an uncertainty of 10% is sufficient. This means that practical applications have different accuracy requirements and so acceptable levels of validation uncertainty are problem dependent. On the other hand, the CFD engineer can influence the numerical uncertainty by changing the simulation setup such as domain size, grid resolution, convergence criteria, turbulence models, etc.

The main question in this paper is whether and how reasonably low levels of uncertainty can be obtained for a wide range of practical applications from maritime industry. To answer this question, we present a selection of cases, performed with MARIN's CFD software ReFRESCO [6, 7], for which uncertainty estimation results are published in the open literature. ReFRESCO solves multi-phase (unsteady) incompressible flows with the RaNS equations, complemented with turbulence models, cavitation models and volume-fraction transport equations for different phases. It is similar to generic commercial CFD codes but only aimed at – and optimized for – maritime applications. It has been verified using the method of manufactured solution [8] and so it is 'ready' for Solution Verification exercises.

The uncertainty procedure is summarized in Section 2 before presenting and analyzing the applications in Section 3. In Section 4 conclusions are drawn on the levels of numerical uncertainty and the circumstances under which these are attained.

2 NUMERICAL UNCERTAINTY ESTIMATION PROCEDURE

The verification and validation procedure is based on research carried out over the past decade by IST. A detailed description is given in [3]. We summarize the procedure in this section.

2.1 Error estimation

At the core of the procedure is an estimator of the discretization error based on the truncated power series expansion

$$\phi_i = \phi_0 + \alpha h_i^p \tag{1}$$

where ϕ_i is a quantity of interest obtained on grid i, ϕ_0 is an estimate of the (unknown) exact value ϕ_{exact}, α is a constant, h_i is the typical cell size of grid i and p is the observed order of grid convergence. Thus, simulation on three different grids is needed to determine the three values ϕ_0, α and p. For cases that comply with all the assumptions behind Equation (1), a verified code will then yield the theoretical order of convergence, typically $p = 2$ for the considered finite volume method, together with the approximation $\phi_i - \phi_0$ of the discretization error $\phi_i - \phi_{\text{exact}}$ on grid i.

For more elaborate cases, however, the theoretical order is not always observed because the underlying assumptions cannot always be satisfied. These assumptions are that:

- the discretization error is significantly larger than the iterative error and/or the round-off error,

- the discretization is the same on every grid (no grid-dependent switches such as limiters),

- the grids are in the asymptotic range (fine enough to justify the truncation of the power series expansion),

- the grids are geometrically similar (the ratio h_i/h_j of two grids is constant in the computational domain).

In practical CFD applications, the round-off error is small enough when the simulation is done in double precision but the iterative error can not always be reduced to the same level. The second assumption is also questionable as various limiters are typically used to avoid spurious oscillations in the numerical solution. The third assumption may require very fine grids that are too costly while the fourth assumption will depend on the capabilities of the grid generation software.

When one or more of these assumptions do not hold, the observed order p can become either unrealistically small ($p < 0.5$) or large ($p > 2.1$) compared to the theoretical order. In that case, several alternative expansions are used that fix the value of p to first or second order or a combination:

$$
\begin{aligned}
\phi_i &= \phi_0 + \alpha h_i \\
\phi_i &= \phi_0 + \alpha h_i^2 \\
\phi_i &= \phi_0 + \alpha_1 h_i + \alpha_2 h_i^2
\end{aligned}
\tag{2}
$$

Furthermore, by using more than three grids, the values ϕ_0, α and p can be determined with weighted or non-weighted least-squares fit that depends on the standard deviation of the fit. The value ϕ is given a larger weight on the finer grids where the best results are expected. The standard deviation of the least-squares fit provides additional information on the quality of the estimator: a low standard deviation implies a good agreement with the power series expansion and hence a reasonable estimation of the discretization error.

Once the discretization error has been estimated, it is combined with a safety factor to yield the uncertainty estimator.

2.2 Uncertainty estimation

The uncertainty estimator U_ϕ is meant to provide a 95% confidence interval:

$$
\phi_i - U_\phi \leq \phi_{\text{exact}} \leq \phi_i + U_\phi
\tag{3}
$$

In our procedure, it depends on the error estimator $\epsilon_\phi = \phi_i - \phi_0$, the standard deviation σ from the least-squares fit and the difference between the actual value ϕ_i and its least-squares fit ϕ_{LS}:

$$U_\phi = \begin{cases} 1.25\epsilon_\phi + \sigma + \|\phi_i - \phi_{LS}\| & \text{for } \sigma < \Delta_\phi \\ 3\frac{\sigma}{\Delta_\phi}\left(\epsilon_\phi + \sigma + \|\phi_i - \phi_{LS}\|\right) & \text{else} \end{cases} \qquad (4)$$

where Δ_ϕ is a measure for the data range defined as

$$\Delta_\phi = \frac{\max(\phi_i) - \min(\phi_i)}{n_g - 1} \qquad (5)$$

where n_g denotes the number of grids. The low safety factor of 1.25 is used when the standard deviation of the least squares fit is relatively small which indicates a good error estimation. Note that the uncertainty estimation procedure reduces to the Grid Convergence Index (GCI) procedure from [1, 2] when the deviation of ϕ_i from the least-squares fit is small. The extra terms are introduced to deal with the scatter and noise that occur in practical applications.

The numerical uncertainty procedure has been thoroughly tested for a variety of cases including turbulent flow over a flat plate and over a backward-facing step and the flow around a tanker, see for example [3, 8, 9] and the references therein. Furthermore, manufactured solutions for turbulent flow, where ϕ_{exact} is known, were used to directly evaluate the quality of the uncertainty estimator [3].

3 UNCERTAINTY IN MARITIME INDUSTRIAL APPLICATIONS

The main question in this paper is whether reasonable levels of uncertainty can also be obtained for a wide range of practical applications with reasonable grid densities. To answer this question, the uncertainty estimation method is applied to various cases from maritime industry, simulated with MARIN's CFD software ReFRESCO.

3.1 Description of the applications

Six different cases are selected to give a fair impression of the different CFD applications for which uncertainty estimation is being done at MARIN and of the typical results that can be expected. The selection covers ships, offshore and navy applications, for Reynolds numbers from model scale $\mathcal{O}(10^6)$ to full scale $\mathcal{O}(10^9)$. All results are published in open literature to which we refer for details.

(a) **LNG carrier** Current loads on a liquefied natural gas (LNG) carrier are computed for model and full scale in [10]. Numerical uncertainty is determined for three current inflow angles in order to establish whether the differences between model and full scale are true scale effects and not tainted by numerics.
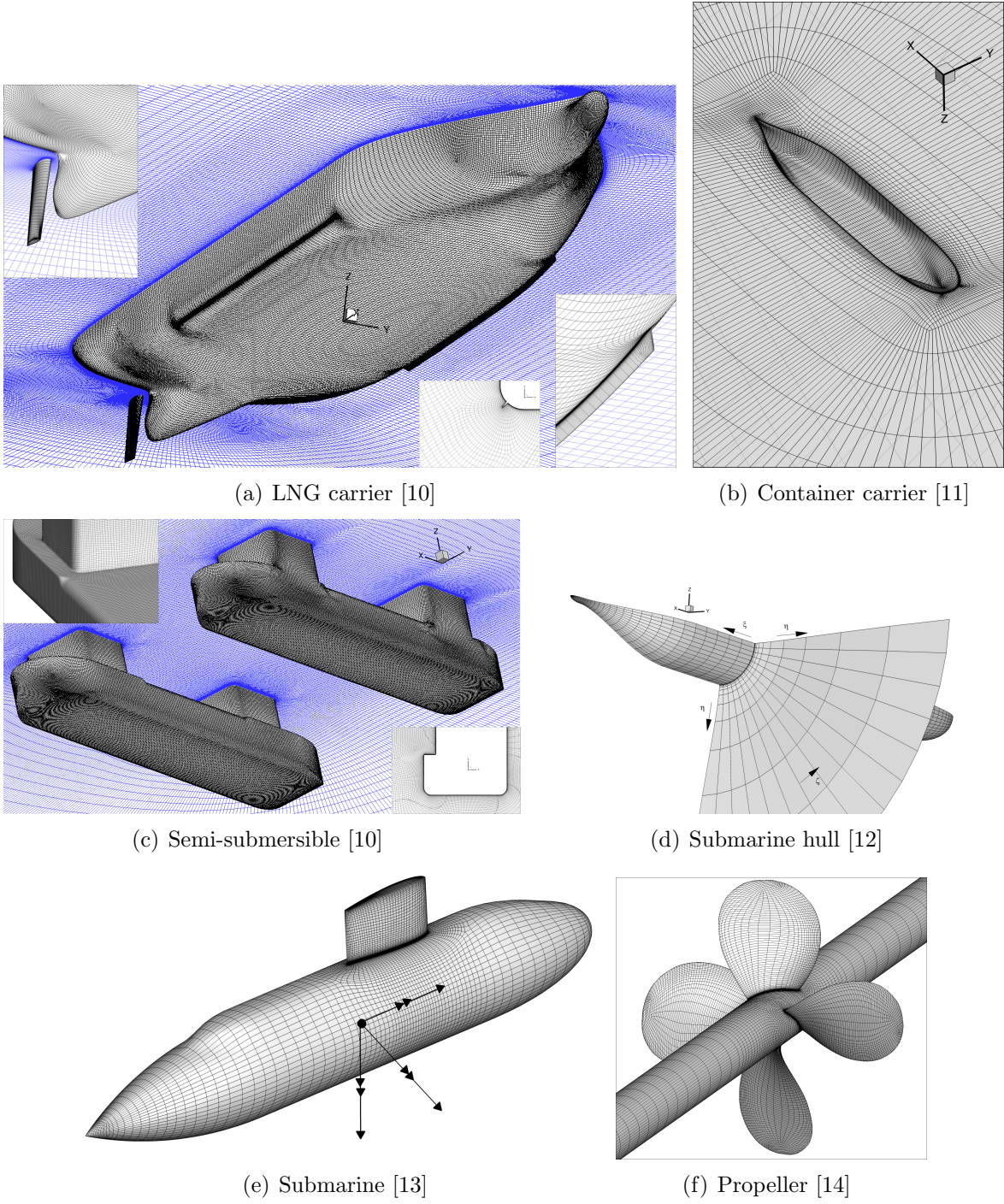
Table 1: Overview of number of grid cells (in millions) used in each application

	Case	Coarsest grid	Finest grid	grids in series
(a)	LNG carrier	0.7	5.7	5
(b)	Container carrier	0.3	5.2	5
(c)	Semi-submersible	1.2	19.3	5
(d)	Submarine hull	0.05	2.8	8
(e)	Submarine	0.11	24.0	9
(f)	Propeller	1.5	24.2	5

(b) Container carrier Maneuvering coefficients are computed in [11] for a container carrier, amongst other cases. Numerical uncertainty is determined for several drift and yaw angles before using the coefficients in a maneuvering simulation program.

(c) Semi-submersible A scale effect study similar to (a) is done for current loads on a semi-submersible at model and full scale in [10].

(d) Submarine hull In [12], maneuvering coefficients are computed for a generic submarine hull at fifteen different inflow angles. Numerical uncertainty is estimated for two inflow angles in order to determine suitable grid densities for this type of application.

(e) Submarine In [13], resistance and pitch moment are computed for a generic submarine in straight flight. Numerical uncertainty is estimated to assess the effect of various grid stretchings towards the hull for two different turbulence models.

(f) Propeller Thrust and torque coefficients are computed in [14] for three propellers in open-water and a range of loading conditions. Numerical uncertainty is determined for one of these propellers, the INSEAN E779A at design condition. This gives useful information on the grid densities needed for other propellers in similar conditions.

3.2 Grid generation

The grids for all six cases have been generated with the package GridPro [15] as it allows the construction of geometrically similar grids, in conformance with the assumption in the error estimator. Figure 1 gives an impression of these grids. The user first generates the finest grid and then obtains the coarser grids in the series by specifying a coarsening factor and the number of grids. A coarsening factor $\sqrt[3]{2}$, for example, roughly halves the total number of cells from one grid to the next. Table 1 shows an overview of the grid densities and the number of grids in a series. Case (d) has the coarsest grids, ranging from 50 thousand cells to 2.8 million; case (f) has the finest grids, ranging from 1.5 million cells to 24.2 million. In all applications, a series of at least five grids is used for the uncertainty estimation; case (e) has the largest series with nine grids.

(a) LNG carrier [10]

(b) Container carrier [11]

(c) Semi-submersible [10]

(d) Submarine hull [12]

(e) Submarine [13]

(f) Propeller [14]

Figure 1: Impression of the block-structured grids used in each application.

3.3 Iterative convergence

The iterative convergence is carefully reported for all cases as it is required that the iterative error is two to three orders of magnitude smaller than the discretization error [9, 16], in accordance with the assumption in the error estimator. The level of convergence, however, is highly case dependent. A drop of at least 5 orders in the residuals of the momentum and mass equations, is attained for cases with weak flow separation, for example a hull at moderate inflow angles or a propeller around design load. When inflow angles are increased and significant flow separation occurs, the residuals still drop 2 or 3 orders before stagnating. However, in such cases, the use of a mathematical model that assumes statistically steady flow is questionable. Nonetheless, the iterative error can affect the estimated uncertainties. Iterative convergence to the level of machine precision is not reported although residual drops of 8 orders are found in case (e) and (f).

3.4 Uncertainty estimation

Since the grids are block-structured and the same coarsening factor is applied in each block and in each direction, the typical cell size h can be defined as $1/\sqrt[3]{N}$ with N designating the total number of cells. Thus, the relative step size between the coarser grids $i > 1$ and the finest grid $i = 1$ becomes

$$\frac{h_i}{h_1} = \sqrt[3]{\frac{N_1}{N_i}} \qquad (6)$$

Figure 2 shows uncertainty estimates representative of the six cases considered. The relative step size is shown on the x-axis of the uncertainty graphs, the y-axis shows the observed quantity of interest ϕ_i as data points together with their least-squares fit. The uncertainty interval is shown for the finest grid at $h_i/h_1 = 1$ and the experimental value, if available, is shown at position $h_i/h_1 = 0$ for comparison.

3.5 Discussion of uncertainty results

The quantity ϕ of interest in case (a) is the force coefficient in the direction perpendicular to the ship for bow-quartering current at full scale with $\mathrm{Re} = 5 \cdot 10^8$. The uncertainty of 2% is quite low for such a large inflow angle. Case (c) shows the same coefficient at a similar inflow angle, only this time at model scale with $\mathrm{Re} = 5 \cdot 10^5$. The uncertainty here is 5.5%, probably because of the blunt shape of the semi-submersible which leads to more extensive flow separation than the slender shape of the LNG carrier. Case (b) shows an uncertainty of 9% in the yaw moment of the container carrier for a non-dimensional yaw rate $\gamma = 0.4$ at model scale with $\mathrm{Re} = 1.2 \cdot 10^7$. Case (d) shows the pressure component of the yaw moment for the submarine hull at a 18° drift angle at model scale with $\mathrm{Re} = 1.4 \cdot 10^7$. Here, the uncertainty is below 1%. Such a low uncertainty is also obtained in case (e) for the resistance coefficient of the submarine in straight flight at model scale with $\mathrm{Re} = 7.5 \cdot 10^5$, but only if the grid is sufficiently stretched towards the wall. The

uncertainty in the thrust coefficient of the propeller case (f) is less than 5% in design conditions (advance ratio $J = 0.747$ and model scale $\text{Re} = 1.7 \cdot 10^6$).

These specific uncertainties were selected from the many results presented in the six references and are neither the worst nor the best; they are meant to give a fair impression of what can be expected in practical applications. For example, Figure 2 shows significant deviation of the data points from the least square fit (scatter), especially in cases (c) and (d). Case (c) shows the largest scatter, even for the finer grids in the series, which illustrates the danger of using only 3 grids for uncertainty estimation. In case (d), the three coarsest grids deviate from the trend and are omitted from the least-squares fit; these grids are clearly not in the asymptotic range assumed by the error estimator. Case (e) illustrates the grid sensitivity of the uncertainty estimator: a clever choice of grid stretching greatly reduces the numerical uncertainty. Cases (b) and (d) also show that the observed order of grid convergence is not necessarily equal to the theoretical order in practical applications. Nonetheless, the overview given in Figure 2 demonstrates that the estimation of the numerical uncertainty in practical applications is not only feasible but also essential.
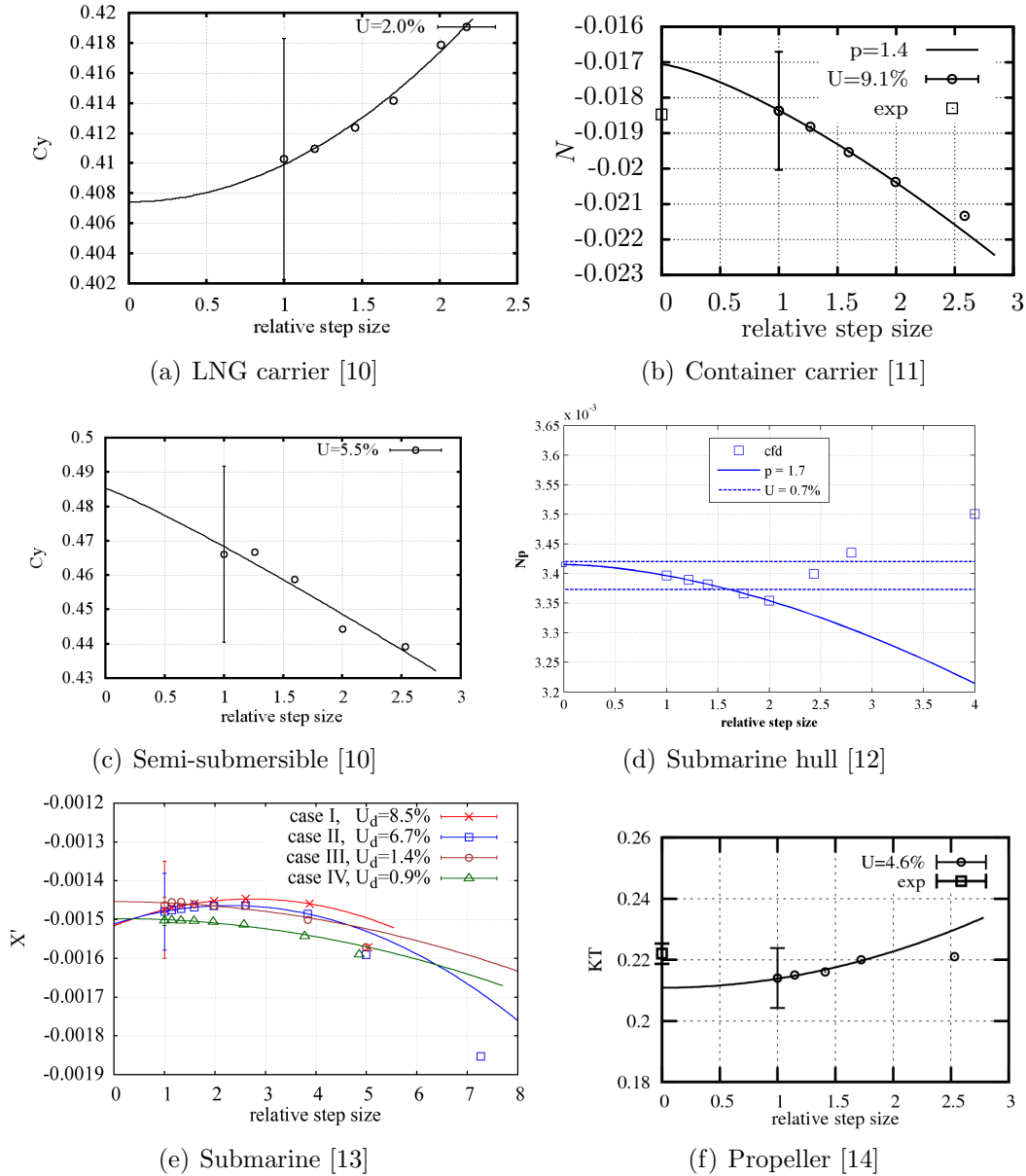
Finally, note that the selection shows a variation in numerical uncertainty from 1% to 9%. A few percent is reasonable for engineering purposes and can be attained for many cases with the current grid generation and CFD tools. It sends a clear message to the CFD engineer to doubt any design 'improvements' of a few percent as well as the meaning of the difference of a single computation with a given experimental result.

4 CONCLUSION

In many of theses cases, numerical uncertainties below 5% are obtained for global quantities such as force coefficients, which is low enough for practical purposes. When available, the experimental values are often within this range, thereby validating the RaNS model for this level of validation uncertainty in these cases. What these cases have in common are highly-refined, block-structured grids, good iterative convergence, and modest inflow angles. When these conditions are not fulfilled, the numerical uncertainty can be higher. These applications clearly show under which circumstances reliable CFD results can be obtained.

Some unsteady RaNS results are presented in [10] without uncertainty estimation. The current uncertainty estimation procedure can be extended to unsteady simulations by considering not only multiple grids, but multiple time-step sizes as well. Doing so adds an order of magnitude to the simulation costs. However, as computational resources continue to grow, this topic can be addressed in the near future. Another direction of future research could be the extension of uncertainty estimation to unstructured, locally refined grids that are increasingly popular in commercial CFD software. This is not trivial as the meaning of asymptotic grid refinement (for a typical cell size $h \to 0$) is lost on unstructured grids that are only refined in local regions of interest.

(a) LNG carrier [10]

(b) Container carrier [11]

(c) Semi-submersible [10]

(d) Submarine hull [12]

(e) Submarine [13]

(f) Propeller [14]

Figure 2: Impression of the uncertainty estimates obtained for the finest grid in each application.

REFERENCES

[1] P.J. Roache. *Verification and Validation in Computational Science and Engineering.* Hermosa Publishers, Albuquerque, New Mexico, 1998.

[2] P.J. Roache. *Fundamentals of Verification and Validation.* Hermosa Publishers, Albuquerque, New Mexico, 2009.

[3] L. Eça and M. Hoekstra. A procedure for the estimation of the numerical uncertainty of CFD calculations based on grid refinement studies. *Journal of Computational Physics*, 262:104–130, 2014.

[4] ASME Committee PTC 61. ANSI standard V&V 20: Guide on Verification and Validation. *Computational Fluid Dynamics and Heat Transfer*, 2009.

[5] C.J. Roy and W.L. Oberkampf. A comprehensive framework for verification, validation, and uncertainty quantification in scientific computing. *Computer Methods in Applied Mechanics and Engineering*, 200(2528):2131–2144, 2011.

[6] G. Vaz, F. Jaouen, and M. Hoekstra. Free-surface viscous flow computations. Validation of URANS code FreSCo. In *Proceedings of ASME 28th International Conference on Ocean, Offshore and Arctic Engineering* [17]. May 31 – June 5, Honolulu, Hawaii.

[7] ReFRESCO webpage. `http://www.marin.nl/refresco`.

[8] L. Eça and M. Hoekstra. Verification and validation for marine applications of CFD. *International Shipbuilding Progress*, 60(1–4):107–141, 2013. Proceedings of 29th Symposium on Naval Hydrodynamics.

[9] L. Eça and M. Hoekstra. Evaluation of numerical error estimation based on grid refinement studies with the method of the manufactured solutions. *Computers and Fluids*, 38:1580–1591, 2009.

[10] A.H. Koop, C.M. Klaij, and G. Vaz. Viscous-flow calculations for model and full-scale current loads on typical offshore structures. In L. Eça, E. Oñate, J. García-Espinosa, T. Kvamsdal, and P. Bergan, editors, *MARINE 2011, IV International Conference on Computational Methods in Marine Engineering*, volume 29 of *Computational Methods in Applied Sciences*, pages 3–29. Springer Netherlands, 2013.

[11] S. Toxopeus. *Practical applications of viscous-flow calculations for the simulation of manoeuvring ships.* PhD thesis, Technische Universiteit Delft, 2011.

[12] S. Toxopeus and G. Vaz. Calculation of current or manoeuvring forces using a viscous-flow solver. In *Proceedings of ASME 28th International Conference on Ocean, Offshore and Arctic Engineering* [17]. May 31 – June 5, Honolulu, Hawaii.

[13] M. Kerkvliet. Influence on the numerical uncertainty of a generic submarine model by changing the wall-normal distribution of the wall-bounded grid cells. In *16th Numerical Towing Tank Symposium*, 2013. 2–4 September 2013, Mülheim, Germany.

[14] D. Rijpkema and G. Vaz. Viscous flow computations on propulsors: verification, validation and scale effects. In *Developments in Marine CFD*. Royal Institution of Naval Architects, 2011. 22–23 March 2011, London, UK.

[15] GridPro webpage. `http://www.gridpro.com`.

[16] L. Eça and M. Hoekstra. On the influence of the iterative error in the numerical uncertainty of ship viscous flow calculations. In *26th Symposium on Naval Hydrodynamics*, 2006. 17-22 September 2006, Rome, Italy.

[17] *Proceedings of ASME 28th International Conference on Ocean, Offshore and Arctic Engineering*, 2009. May 31 – June 5, Honolulu, Hawaii.